THE JOURNAL OF PHYSICAL CHEMISTRY C

Article

Controlling Carboxyl Deprotonation on Cu(001) by Surface Sn Alloying.

Alvaro Carrera, Lucila J. Cristina, Silvina Bengió, Albano Cossaro, Alberto Verdini, Luca Floreano, Javier Daniel Fuhr, Julio Esteban Gayone, and Hugo Ascolani

J. Phys. Chem. C, **Just Accepted Manuscript** • DOI: 10.1021/jp404983n • Publication Date (Web): 23 Jul 2013

The Journal of Physical Chemistry C is published by the American Chemical Society. 1155 Sixteenth Street N.W., Washington, DC 20036

Controlling Carboxyl Deprotonation on Cu(001) by Surface Sn Alloying

A. Carrera,[†] L. J. Cristina,[†] S. Bengió,[†] A. Cossaro,[‡] A. Verdini,[‡] L. Floreano,[‡] J. D. Fuhr,[†] J. E. Gayone,[*,†] and H. Ascolani[*,†]

Centro Atómico Bariloche, CNEA, and CONICET, Av. E. Bustillo 9500, R8402AGP, Bariloche, Argentina., and CNR-IOM, Laboratorio TASC, Basovizza SS14 Km. 163.5, I-34149 Trieste, Italy,

E-mail: gayone@cab.cnea.gov.ar; ascolani@cab.cnea.gov.ar

[*]To whom correspondence should be addressed
[†]Centro Atómico Bariloche
[‡]CNR-IOM

July 10, 2013

Abstract

We find that for adsorbed terephthalic acid (TPA) molecules, surface Sn alloying deactivates the Cu(001) surface by decoupling the adsorbed molecules from the substrate. This effect is investigated for the case of the 0.5 ML phase of the Sn/Cu(001) surface alloy by applying fast X-ray Photoemission Spectroscopy, Scanning Tunneling Microscopy, Near-Edge X-ray Absorption Fine Structure spectroscopy and Density Functional Theory calculations. The experimental results conclusively show that the deprotonation reaction of the carboxyl groups occurring in the clean Cu(001) is fully inhibited on this Sn/Cu(001) surface alloy, which allows the molecules to form two-dimensional arrays stabilized by [OH$\cdots$O] hydrogen bonds. The formed arrays exhibit a crystal structure that is practically indistinguishable from that theoretically obtained for unsupported TPA sheets, suggesting an extremely weak molecule/substrate interaction. This is supported by DFT calculations of the adsorption energy landscape of the TPA sheets formed on the Sn/Cu(001) template: the lateral variation of the adsorption energy (corrugation) is estimated to be less than 0.2 eV, with an adsorption energy per molecule in the range 1.6-1.8 eV and a contribution of each double [OH$\cdots$O] bond of 1 eV. Finally, the performed thermal desorption experiments show that the TPA sheets remain stable on the surface alloy until their desorption. From these experiments, a value of 1.5 eV was determined for the desorption energy barrier, which is consistent with the important contribution of the [OH$\cdots$O] bonds to the stability of the sheets as theoretically predicted. The results reported in this study suggest that a gradual activation of the interaction between the TPA molecules and the Cu(001) surface will also be obtained for decreasing Sn coverage.

KEYWORDS: TPA, Adsorption, Desorption, Hydrogen, Bond.

Introduction

The production of laterally-nanostructured supramolecular architectures on metallic surfaces has received considerable attention in the last few years for both single [1–3] and mixed components.[4,5] Specially interesting are the two-dimensional networks based on hydrogen bonds and metal-ligand interactions since these systems would have a wide range of applications in organic electronic,[6] magnetic devices,[7,8] catalysis,[9] etc. An effective route to control the intermolecular assembly is that of employing molecules with terminations suitably functionalized to match the electron affinity of neighboring companions.[4,5,10,11] In any case, the interaction of the terminal groups with the substrate plays a crucial role affecting the molecular self-assembly as well as the chemical and electronic properties of the resulting interfaces.[12–15] In this article we present the Sn/Cu(001) surface alloy as a novel and adaptable template for the formation of H-bonded organic structures. In fact, Sn alloying was previously reported to affect the chemical reactivity of Pt [16–23] and Pd [24–26] surfaces. Here we show that the Sn/Cu(001) alloying effectively decreases the substrate reactivity, hence dramatically changing the energy landscape of molecular adsorption and intermolecular bonding.

At room temperature (RT), Sn atoms deposited on Cu(001) surfaces replace the Cu atoms in the outmost substrate layer producing a bimetallic surface alloy. The alloying effect occurs for Sn submonolayer coverage up to 0.5 monolayer (ML) giving rise to a variety of commensurated phases.[27] In order to test the proposed substrate, we analyzed the adsorption and self-assembly properties of terephthalic acid (TPA) molecules on the phase formed at 0.5 ML. In this phase (see Figure 1), the Sn:Cu composition of the outmost layer is not 1:1 but 3:2 due to the formation of Cu vacancies. At room temperature (RT), the vacancies are ordered forming rows oriented along the $< 100 >$ crystallographic directions, causing a $(3\sqrt{2}\times\sqrt{2})R45^\circ$ reconstruction.[28] It is also worth noting that this reconstruction undergoes a reversible order-disorder transition to a $(\sqrt{2}\times\sqrt{2})R45^\circ$ phase when the temperature increases above 360K, which is related to the disordering of the Cu vacancies.[29,30]

TPA can be regarded as the basic building block of rod-like polybenzene dicarboxylic

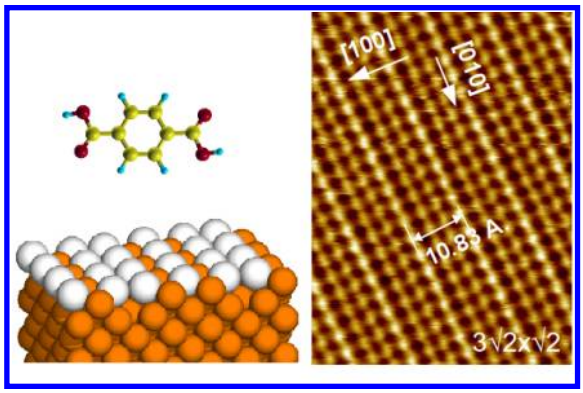

Figure 1: Left: Schematical drawings of a TPA molecule and of the $(3\sqrt{2} \times \sqrt{2})R45°$ reconstruction formed by 0.5 ML of Sn atoms (white-grey) on the Cu(001) substrate (orange). Right: Filled-state STM image of the $(3\sqrt{2} \times \sqrt{2})R45°$ phase taken with a bias voltage of -0.05 V and a reference current of 2 nA. Only the Sn atoms are seen.

acids, a family of molecules which has been widely used as linkers to build interesting two-dimensional (2D) supramolecular structures.[7,31] The versatility of these molecules is strongly related to the properties of the carboxyl groups (RCOOH). While on Cu(001) surfaces only a small fraction of carboxyl groups remains protonated at RT,[12–14] on Au(111) surfaces[32,33] and on a graphene layer grown on Ni(111)[34] the TPA molecules remain neutral forming H-bonded sheets. This work shows that the main effect of Sn alloying is to reduce the chemical reactivity of the Cu(001) surface with respect to the carboxyl groups to such an extent that the deprotonation reaction observed on the bare substrate is fully inhibited. TPA molecules are then left free to organize into regular arrays stabilized through intermolecular hydrogen bonds.

Methods

The experiments of Scanning Tunneling Microscopy (STM) were carried out at the Centro Atómico Bariloche, Argentina, using an ultra-high vacuum system from Omicron-Nanotechnology. The preparation of the $(3\sqrt{2} \times \sqrt{2})R45°$ phase and the deposition of the TPA molecules were carried out by following the same procedures described in our previously-publised works.[14,28] All the STM images reported in this work were taken at RT using W tips.

The experiments of X-ray Photoelectron Spectroscopy (XPS) and of Near-Edge X-ray Adsorption Fine Structure (NEXAFS) spectroscopy were carried out at the ALOISA beam line[35] of the ELETTRA synchrotron, at Trieste. The XPS spectra, taken with a photon energy of 655 eV, were measured at grazing incidence (4°) and in normal emission by means of a hemispherical electron analyzer with angular acceptance of 2° and an overall energy resolution of 250 meV. Four energy windows centered on the regions of the Fermi edge and the Cu 3p, C 1s and O 1s core levels, were typically acquired by means of a 2D delay-line detector.[36] The desorption curves were obtained by monitoring during sample annealing the corresponding core level in snap-shot acquisition mode, which requires a lower kinetic energy resolution (600 meV) to collect the whole core level peak profile within a single shot (2 sec) of the 2D detector.

NEXAFS spectra at the carbon K-edge have been taken by means of partial electron yield with a channeltron facing the sample and a negatively biased grid in between for rejecting low energy secondary electrons (bias of -250 V). The photon energy resolution was set to about 75 mV. Absolute energy calibration has been obtained a posteriori through the carbon absorption signal observed in the I_0 drain current, as measured on the metal coating of the refocusing mirror, that was independently calibrated by simultaneous acquisition of the gas phase absorption spectra from CO.[37] The spectra have been collected by keeping the sample at constant grazing angle of 6 degrees, while rotating the surface around the photon beam axis in order to switch from Transverse Magnetic ('p') to Transverse Electric ('s') polarization. Further details about the scattering geometry can be found in Ref.[35] To compensate for the variation of the photon flux across the K-edges, we have normalized the NEXAFS spectra from the TPA overlayer to the spectra taken from the bare Sn/Cu(001) substrate.

The calculations based on the Density Functional Theory (DFT) were performed using the QUANTUM ESPRESSO package,[38] which is an implementation of the plane-wave with ultrasoft-pseudopotentials approach. The exchange-correlation effects were treated using the

second version of van der Waals density functional (vdW-DF)[39–42] with improved exchange.[43] For the surface calculations we have used the slab method, with five Cu layers with the Sn alloy in the topmost layer. For all the calculations, we fixed the two lower layers while all other atoms are allowed to relax. We used a wave-function/charge cutoff of 30/300 Ry, and Brillouin integrations were done using a grid equivalent to $12\times12\times1$ k-points for the surface unit cell. For a given configuration corresponding to N molecules adsorbed on the surface, the mean adsorption energy per molecule is calculated by

$$E_{\rm ads}({\rm TPA}) = -\left[\frac{E_{\rm total} - E_{\rm surface} - N_{\rm H}E_{\rm ads}({\rm H})}{N} - E_{\rm TPA}\right] \quad (1)$$

where: $E_{\rm total}$ is the total energy of the system with the adsorbed molecules; $E_{\rm surface}$ is the total energy of a clean surface with the same area; $N_{\rm H}$ is the number of dissociated H atoms; $E_{\rm ads}({\rm H}) = 0.18$ eV corresponds to adsorption energy of H atoms on a clean Cu(001) surface; and $E_{\rm TPA}$ is the total energy of an isolated TPA molecule.

Results and Discussion

To characterize the adsorption properties of the TPA molecules deposited onto the $(3\sqrt{2}\times\sqrt{2})R45^\circ$ phase from the chemical point of view, we measured high-resolution XPS spectra of the O1s and C1s core levels. Figure 2(a) shows a representative O1s spectrum of a sample prepared by depositing less than 1 ML of molecules onto the Sn alloyed Cu(001) surface kept at RT. The spectrum shows the typical double-peak lineshape produced by the two inequivalent oxygen of the carboxyl groups.[44] Specifically, the peaks at 533.6 and 532.3 eV correspond to the OH and C=O groups, respectively. In addition, the shift of 1.3 eV between these peaks indicates that the carboxyl groups are forming [OH$\cdots$ O] hydrogen bonds.[44,45] Therefore, this O1s spectrum reveals that, in contrast to the case of the bare Cu(001) surface, all the TPA molecules remain complete at RT and interacting through hydrogen bonding. The same conclusion can be derived from the corresponding C1s spectra

(See the Supplementary Information, SI).

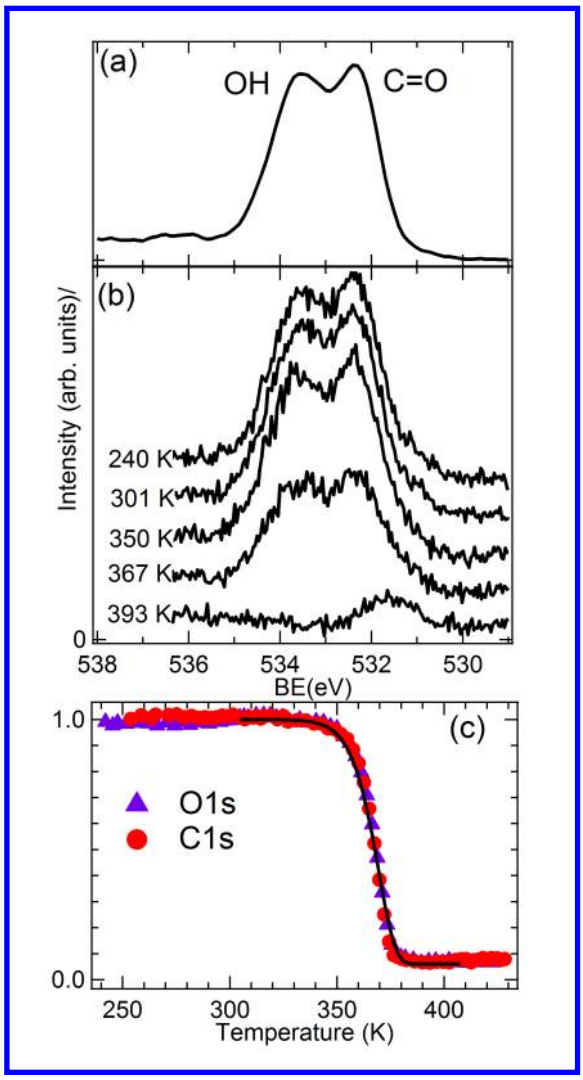

Figure 2: a) O1s photoemission spectra obtained for a submonolayer coverage of TPA on the 0.5 ML Sn/Cu surface alloy at room temperature b) series of O1s spectra measured as a function of the substrate temperature using a fast-XPS mode. c) Total intensity of the O1s and C1s spectra vs substrate temperature. The continuos black line corresponds to a first-order Polanyi-Wigner model (see text and the SI).

To investigate the stability against deprotonation of the carboxyl groups of the TPA molecules adsorbed on the 0.5 ML Sn/Cu(001) surface alloy, we measured the O1s and C1s core levels as a function of substrate temperature; we started from a sample prepared at 240K with a heating rate of approximately 40 K/min. It is worth mentioning that the evolution of each core level was independently obtained from different samples. Figure 2(b) shows four

O1s spectra that are representative of the whole O1s series measured in real time during the annealing of the sample, where the first spectrum corresponds to the sample as prepared. We note that the initial double-peak structure is clearly observable in the spectrum recorded at 367K even when it shows a significant decrease of intensity. In contrast, the spectrum corresponding to 393K indicates a totally different situation. There is a single peak with an intensity of about 5% of the initial one. This spectrum shape remains unchanged as the temperature increases until 430K. Importantly, the $(3\sqrt{2} \times \sqrt{2})R45°$ reconstruction was found to survive the thermal desorption experiment, as follows from the RHEED pattern observed after the TPA desorption.

The results of the thermal desorption experiments are summarized in Figure 2(c) where the normalized intensities of both the O1s and C1s core-level photoemission spectra are shown as a function of the substrate temperature. Notably, although the curves were obtained from different samples, the evolution of the C1s intensity with temperature coincides with that of the O1s, indicating that the molecules remain complete during the experiment. Therefore, the transition observed at (370±5) K corresponds to the desorption of neutral TPA molecules. The residual O and C atoms correspond to fully deprotonated molecules adsorbed on the surface, as deduced from the analysis of both the O1s and the C1s core levels; we attribute these deprotonation events to defects of the surface alloy. In conclusion, the XPS data reveal that deposition of 0.5 ML of Sn on the Cu(001) surface completely inhibits the deprotonation reaction of the carboxyl groups.

By fitting the desorption curve (see SI) with a first-order model we obtain an activation energy for desorption of 1.51 eV and a rather high frequency-factor ν of $3 \times 10^{19} s^{-1}$.[46] Values of ν higher than $10^{13} s^{-1}$ have been previously reported for organic molecules and, according to the transition state theory, is related to an increase of the entropy when they are going from the adsorbed state to the gas-phase state (transition state).[47] In this sense, the obtained ν could be ascribed to the rather strong and directional H-bonds that could hinder some of the translation and rotational movements of the molecules in the adsorbed layer.[48,49] Once

the molecule is desorbed, it can move freely, resulting in an increase of the entropy with respect to the adsorbed state.

Figure 3(a) compares the NEXAFS carbon spectra obtained with p and s polarization from a sample with a submonolayer amount of TPA molecules deposited at 300K on the Sn/Cu(001) template. The peaks at 284.6 and 285.5 eV observed in the spectrum measured in Transverse Magnetic polarization correspond to π^* resonances of the aromatic ring, while those in the region between 287-290 eV are attributed to carboxyl groups.[45,50] The polarization dependence of the π^* resonances clearly shows that the molecules are adsorbed with the C-ring plane parallel to the surface.[50]

It is interesting to compare the carbon NEXAFS spectrum obtained with p-polarization from the TPA/Sn/Cu(001) system with the corresponding one measured on the 3×3 phase formed by TPA molecules on the bare Cu(001) surface (see Figure 3(b)). The 3×3 phase is formed by fully deprotonated TPA molecules strongly bound to the substrate through four Cu-O bonds.[13,14] We firstly note that, while in the TPA/Sn/Cu(001) system the π^* resonances are clearly resolved, in the 3×3 phase are not. Thus indicating a stronger molecule/substrate interaction in the latter case.[50] Secondly, there are also notable differences in the region of the carboxyl groups, which supports the hyphothesis of neutral TPA molecules adsorbed on the Sn/Cu(001) template.

STM images of a sample produced at RT are shown in Figure 4. Panel (a) shows a region where large molecular islands are present. Notice that all the areas surrounding the molecular islands show the typical pattern of stripes oriented along the [100] crystallographic direction stemming from the $(3\sqrt{2} \times \sqrt{2})R45^\circ$ reconstruction,[28] which is another evidence that the substrate template is stable against to TPA adsorption. Two different types of molecular islands, that are labelled A and B in the image, can be identified. Fig. 4(b) shows an isolated A-type island starting from monoatomic surface steps. The apparent height of the molecular island with respect to the substrate is 1.47 Å; we remark that this value is clearly larger than 1.0 Å, the value obtained for the 3×3 phase of deprotonated TPA

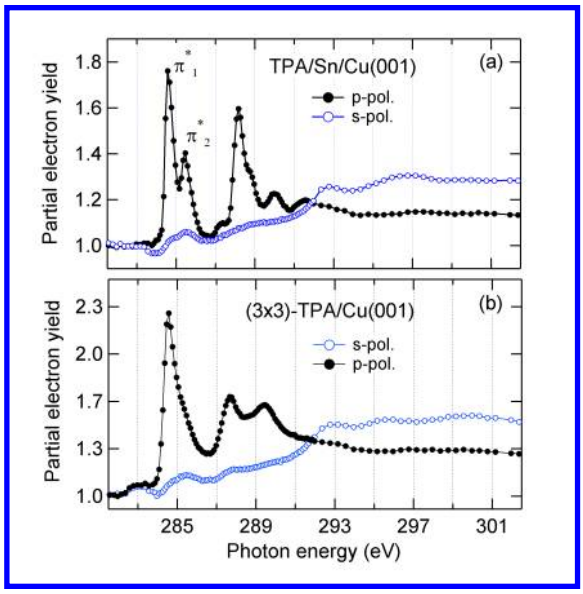

Figure 3: a) Absorption carbon K-edge spectra recorded at 200K of a TPA/Sn/Cu(001) surface prepared at 300K. b) Absorption carbon K-edge spectra recorded at 300K of the 3x3 phase formed by TPA molecules on the bare Cu(001) substrate.

molecules on bare Cu(001) surfaces under identical tunneling conditions. As can be seen, this island has straight edges and ribbon shape indicating a preferential direction of growth. Again, the characteristic stripes of the surface alloy are clearly visible on the uncovered portion of the terraces. Finally, Figure 4(c) shows a zoom of the B-type island observed in Fig. 4(a). In this image, one out of three molecular rows along the [100] crystallographic direction looks brighter suggesting that the B-type molecular structure is conmensurated with the $(3\sqrt{2} \times \sqrt{2})R45^\circ$ reconstruction along the mentioned direction. Apparently, there is a bright molecular row every two substrate stripes. Taking the XPS, STM and NEXAFS data into consideration, we conclude that the TPA molecules form H-bonded sheets on the $(3\sqrt{2}\times\sqrt{2})R45^\circ$ reconstruction, similarly to those formed by the molecules on the Au(111).[32] Moreover, we conclude that the different island types are originated by different orientations of the TPA sheets with respect to the substrate.

Figure 5 shows schematic models for the TPA islands observed in Figure 4. It is clear from Figure 4(b) that, in the case of the A-type islands one of the vectors of the unit cell, $\vec{a}_2$, is parallel to the [010] crystallographic direction, whereas the other one, $\vec{a}_1$, forms an

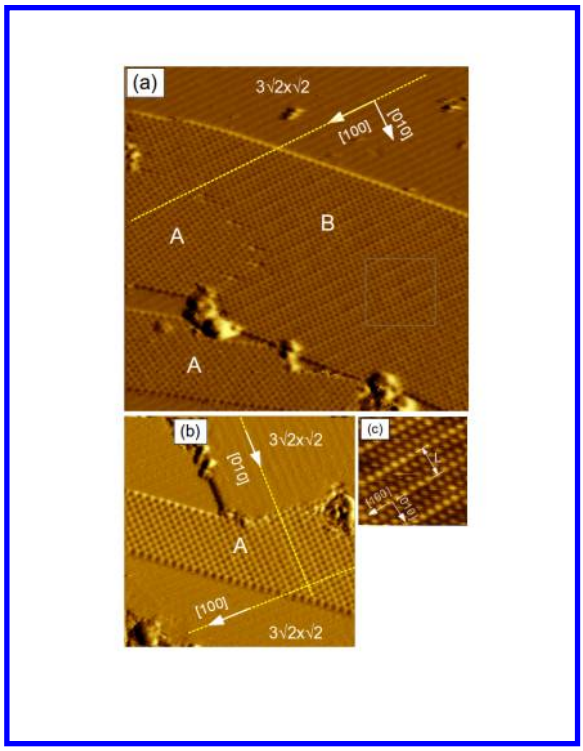

Figure 4: Filled-state STM images TPA molecules adsorbed on the the $(3\sqrt{2} \times \sqrt{2})R45°$ phase of the Sn/Cu(001) surface alloy. The square superimposed to the B-type island in panel a) corresponds to the area zoomed in c). Image sizes: a: (500×500)Å^2; b: (250×250)Å^2 c: (100×100)Å^2. Conditions: V=-2V /I= 10pA. The apparent-height of the islands with respect to the substrate is, in average, ~ 1.5 Å .The distance L indicated in c) between two bright molecular rows is 22.5 ± 1 Å.

angle of about 10° with respect to the [100] direction. The crystallographic structure of the A-type islands can be determined with good precision from this STM image, where the two inequivalent 90°-rotated domains of the $(3\sqrt{2} \times \sqrt{2})R45°$ substrate reconstruction are seen; here, the corresponding stripes were used to calibrate the STM scanner along both the [100] and the [010] crystallografic directions. We found that the unit-cell vectors have very similar length, (7.50 ± 0.2)Å , and that the subtended angle is $(81 \pm 2)°$. In addition, the distance $|\vec{b} = \vec{a}_1 - \vec{a}_2|$ between the centers of the C rings corresponding to consecutive molecules interconnected through [OH$\cdots$O] bonds was also independently determined, obtaining a value of (9.70 ± 0.2)Å . We note that the obtained $|\vec{b}|$ length is slightly larger than the value reported for TPA bulk (9.54 Å)[51] but, in turn, clearly smaller than the value reported for

TPA sheets formed on Au(111)[32] (around 10 Å).

On the other hand, the B-type islands are related to the A-type ones by a $\sim 10^{\circ}$ azimuthal rotation that leaves the $\vec{a}_1$ vector aligned with the [100] crystallographic direction (see Figure 5). Compared to the A-type configuration, we have not detected any significant difference in the crystallographic parameters apart from the mentioned rotation. Additionally to the A- and B- types, other orientations were observed, in particular, islands where hydrogen bonds are oriented perpendicular and parallel to the stripes of the substrate (not shown). The observation of multiple sheet orientations strongly suggests a smooth potential landscape for the interaction between the TPA molecules and the substrate.

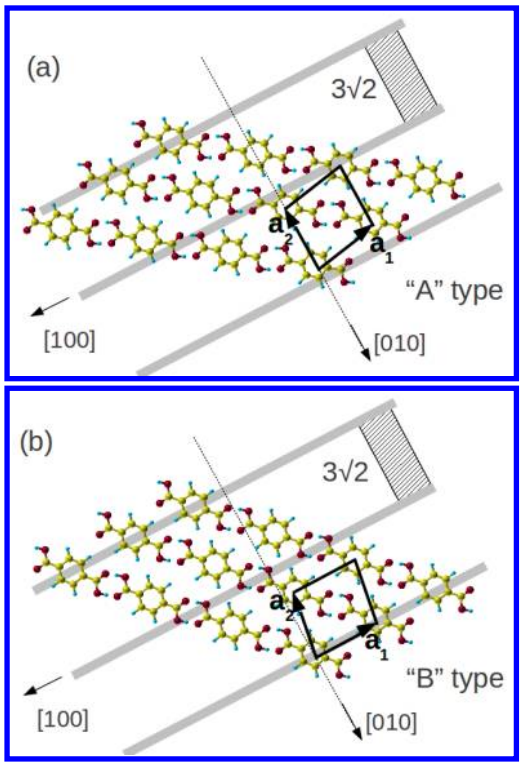

Figure 5: Schematic models illustrating the different observed orientations of the TPA sheets on the 0.5 ML Sn/Cu(001) surface alloy. The dashed rectangles represent the $(3\sqrt{2}\times\sqrt{2})R45^{\circ}$ unit cell of the substrate. The thick grey lines represent the observed stripe pattern produced by the reconstruction in the STM images. As can be seen in Fig. 5 of Ref.,[28] the stripes correspond to rows of Sn atoms that are slightly elevated with respect to the other Sn rows along the [100] direction. In the B-type configuration, one every three molecular row along this crystallographic direction would be adsorbed with the C-rings atop the elevated Sn atoms (see the SI).

We carried out DFT calculations in order to gain a deeper understanding on the origin of the decoupling effect between the adsorbed molecules and the Cu(001) substrate observed in the TPA/Sn/Cu(001) system.

We first relaxed the crystallographic structure of an unsupported 2D sheet of TPA molecules obtaining values of 7.43 Å and 79.5° for the length of the unit-cell vectors and for the subtended angle, respectively. These values are in excellent agreement with the structural parameters experimentally determined for a A-type sheet confirming that the interaction of the TPA molecules with the Sn/Cu(001) substrate is extremely weak. In addition, the calculated formation energy of the unsupported 2D sheet of TPA molecules turned out to be 1.04 eV per molecule.

We then evaluated the adsorption of isolated TPA molecules on the $(3\sqrt{2} \times \sqrt{2})R45°$ reconstruction illustrated in Fig. 1. This reconstruction allows for many non-equivalent adsorption sites on the surface. We considered two main adsorption sites, on top of a surface atom site (Sn or Cu) and a hollow site, and also two orientations, [100] and [110]. For each initial configuration the system is allowed to relax, and the adsorption energy is calculated using Eq. (1). In Fig. 6 we show several of the final relaxed configurations obtained for neutral molecules with the corresponding adsorption energies. We found that the slightly preferred adsorption site is on top of a surface atom, with and an adsorption energy in the range 0.76-0.78 eV, depending weakly on the surface atom on top of which is located the TPA molecule, and on the molecule orientation. For the isolated TPA molecule, the adsorption energy is greatly reduced with respect to the 2.04 eV calculated for TPA adsorbed on the bare Cu(001) surface.[14] We also note that the adsorption-energy value obtained for isolated TPA molecules on the Sn alloyed Cu(001) surface is comparable to the values calculated for different aromatic molecules adsorbed on Au(111) (benzene: 0.55 eV, pyridine: 0.48 eV, thymine: 0.67 eV, cytosine: 0.77 eV).[52] This suggests that the analyzed phase of the Sn/Cu(001) surface alloy displays a reactivity to TPA comparable to that of Au(111).

Additionally, we estimated the corrugation of the adsorption energy landscape seen by neutral molecules. To this purpose we performed a barrier calculation for the diffusion of a TPA molecule from the first configuration in Fig. 6 to a site on top of a neighbor Sn surface atom. This calculation was done using the nudge elastic band (NEB) method to obtain the saddle point configuration and energy. A diffusion barrier of 0.15 eV was obtained, resulting in a saddle point adsorption energy of 0.62 eV. For the considered configurations E_{ads} varies then in the range 0.62-0.78 eV. The corrugation of the adsorption energy landscape seen by an isolated neutral TPA molecule is then estimated to be lower than 0.20 eV. On the other hand, on the bare Cu(001) surface, the difference in E_{ads} for the TPA molecule adsorbed in its preferred adsorption geometries, i.e. aligned in the [100] or [110] directions, is already 0.20 eV.[14] Therefore, we can conclude that not only the adsorption energy but also the energy landscape corrugation is greatly reduced by the Sn alloying.

The adsorption energies of a deprotonated and a semi-deprotonated molecules were also calculated obtaining 0.17 eV and -0.52 eV, respectively. The deprotonation of the TPA molecule on the $(3\sqrt{2} \times \sqrt{2})R45°$ reconstruction is therefore energetically unfavorable, contrary to what was found on the bare Cu(001) surface.

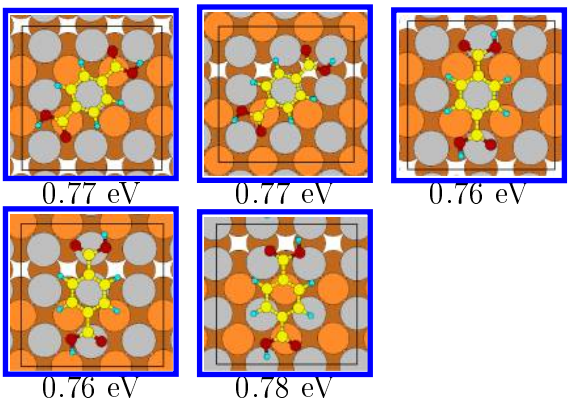

Figure 6: Several of the final relaxed for a TPA molecule adsorbed on the $(3\sqrt{2} \times \sqrt{2})R45°$ reconstruction of 0.5 ML of Sn on Cu(001), together with the corresponding adsorption energies. Sn atoms in the top layer are shown in gray, while Cu atoms in the top and second surface layers are shown in light and dark brown respectively.

As the 2D sheet of TPA molecules is not conmesurated with the substrate, a calculation

of the supported sheet is not feasible. For an estimation of its formation energy, we first carried out a calculation with a configuration containing two molecules forming H-bonds. This configuration is shown in Fig. 7. The calculated adsorption energy for both molecules is 2.52 eV. Subtracting from this value twice the adsorption energy calculated for isolated TPA molecules, a value of $\sim$ 1 eV is obtained for the interaction energy between molecules. This value is close to the calculated formation energy for the unsupported 2D sheet (1.04 eV), which means that the H-bonds are only slightly weakened by the presence of the substrate. Assuming that intermolecular interaction is largely dominated by the [OH$\cdots$O] hydrogen bonds, we conclude that the formation energy of a double H-bond on the surface is about 1 eV.

Finally, the energy per molecule in a H-bonded sheet of absorbed TPA molecules can thus be estimated by adding the obtained formation energy of a double H-bond to the adsorption energy of an isolated molecule. We therefore estimate the adsorption energy per molecule in a H-bonded TPA sheet to be in the range 1.60-1.80 eV. These values compare very well with the experimentally-determined value of the desorption energy (1.5 eV), indicating that there are no extra energetic barriers for the desorption of TPA molecules from the studied Sn/Cu(001) surface alloy. The contribution of the [OH$\cdots$O] interaction to the stability of the adsorbed TPA sheets can be also put in evidence by comparing the desorption-energy value determined in this work with the desorption energies reported for similar molecules that do not form [OH$\cdots$O] bonds. For benzene adsorbed on Au(111) [53] and hexane adsorbed on graphite,[47] desorption energies of 0.64 eV and 0.76 eV, respectively, were derived from thermal desorption experiments. These low values strongly support that the [OH$\cdots$O] bonds are the main responsible for the stability of the TPA sheets.

From the theoretical and experimental results discussed above we show that the subnetwork of Sn atoms deactivates the Cu(001) surface by decoupling the adsorbed molecules from the Cu(001) substrate. As mentioned in the introduction, the decrease of surface reactivity by Sn alloying has already been reported for Pt and Pd surfaces. The origin of this effect can

be attributed to the lower reactivity of Sn atoms in the surface alloy, as well as to a steric effect that hinder the interaction of the molecule with the Cu atoms in the top surface layer. Thus, a gradual activation of the interaction between the TPA molecules and the Cu(001) surface can be expected for decreasing Sn coverage when Cu atoms in the surface began to be exposed to the vaccum.

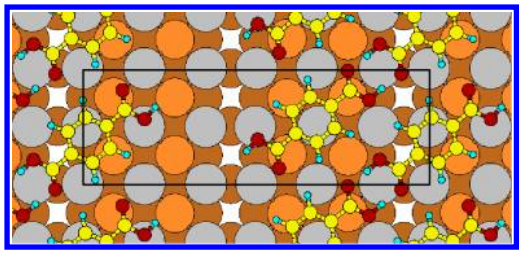

Figure 7: Configuration containing two molecules forming H-bonds used to estimate the bonding energy between molecules in the adsorbed TPA sheet. Sn atoms in the top layer are shown in gray, while Cu atoms in the top and second surface layers are shown in light and dark brown respectively.

Conclusions

We find that the subnetwork of Sn atoms contained in the top surface layer of the $(3\sqrt{2} \times \sqrt{2})R45°$ reconstruction of the 0.5 ML Sn/Cu(001) surface alloy causes a drastic reduction of the interaction between the TPA molecules and the Cu(001) substrate. The effect is important enough to cause the complete inhibition of the deprotonation reaction of the carboxyl groups, a process that is already active at RT on the bare Cu(001) surface. Therefore, the deposition of 0.5 ML of Sn atoms allows to switch the self-assembling properties of TPA molecules from those observed on Cu(001) to those found on Au(111). The neutral molecules form ordered 2D arrays stabilized by [OH$\cdots$O] bonds which is practically indistinguishable from that theoretically obtained for unsupported TPA sheets.

The thermal desorption experiments show that the TPA sheets remain stable on the surface alloy until the thermal energy is large enough for the activation of their desorption. Remarkably, the $(3\sqrt{2} \times \sqrt{2})R45°$ reconstruction was systematically found after the TPA

desorption. From these experiments we determined a desorption energy of 1.5 eV and a frequency-factor ν of $3 \times 10^{19} s^{-1}$. The experimentally determined desorption energy compares very well with the theoretically estimated adsorption energy (1.6-1.8 eV per molecule) suggesting that there are no energy barriers along the desorption pathway of the molecules. The contribution of the [OH$\cdots$O] interaction to the adsorption energy was theoretically estimated to be $\sim$1 eV. On the other hand, the high value obtained for the frequency-factor is ascribed to the rather strong and directional H-bonds that could hinder some of the translation and rotational movements of the molecules in the adsorbed layer.

Finally, our finding strongly suggests that the 0.5 ML Sn/Cu(001) surface alloy would be a suitable substrate template to produce two-dimensional H-bonded networks at RT based on carboxyl groups.[54,55] We thus think that Sn alloying can be a valuable route for tailoring the Cu(001) surface to the requirements of two-dimensional H-bonded networks based on carboxyl groups.

Acknowledgments

We thank Mr. Lucas Lopez for valuable technical assistance and Prof. Oscar Grizzi for a critical reading of the manuscript. We acknowledge financial support by the following Argentine institutions: CONICET (PIP 112 200801 00958), J.A. Balseiro and ANTORCHAS foundations, and ANPCYT (PICT2005/33432, PME 2003/118), UNCuyo(Grants 06/C390). We also acknowledge financial support from the ICTP-ELETTRA USERS PROGRAMME. We also thank CONICET for the fellowships of L.J.C. Four of us, S.B., J.D.F., J.E.G. and H.A. are members of CONICET of Argentina.

Supporting Information

The C1s photoemission spectra corresponding to TPA/SnCu(001) samples prepared at 300 and 240K together with details of the analysis of the thermal-desorption curves are reported.

This information is available free of charge via the Internet at http://pubs.acs.org.

References

(1) Barth, J. V.; Costantini, G.; Kern, K. Engineering atomic and molecular nanostructures at surfaces. *Nature* **2005**, *437*, 671–679.

(2) Barth, J. V. Molecular Architectonic on Metal Surfaces. *Annual Review of Physical Chemistry* **2007**, *58*, 375–497.

(3) Elemans, J. A. A. W.; Lei, S.; de Feyter, S. Molecular and Supramolecular Networks on Surfaces: From Two-Dimensional Crystal Engineering to Reactivity. *Angew. Chem. Int. Ed.* **2009**, *48*, 7298–7332.

(4) Sedona, F.; Marino, M. D.; Sambi, M.; Carofiglio, T.; Lubian, E.; Casarin, M.; Tondello, E. Fullerene/Porphyrin Multicomponent Nanostructures on Ag(110): From Supramolecular Self-Assembly to Extended Copolymers. *ACS Nano* **2010**, *4*, 5147.

(5) de Oteyza, D.; Garcia-Lastra, J.; Corso, M.; Doyle, B.; Floreano, L.; Morgante, A.; Wakayama, Y.; Rubio, A.; Ortega, J. Balancing Intermolecular and Molecular Substrate Interactions in Supramolecular Assemblies. *Adv. Func. Mat.* **2009**, *19*, 1.

(6) Gonzalez-Lakunza, N.; Fernández-Torrente, I.; Franke, K. J.; Lorente, N.; Arnau, A.; Pascual, J. I. Formation of Dispersive Hybrid Bands at an Organic-Metal Interface. *Phys. Rev. Lett.* **2008**, *100*, 156805.

(7) Gambardella, P.; Stepanow, S.; Dmitriev, A.; Honolka, J.; de Groot, F. M. F.; Lingenfelder, M.; Gupta, S.; Sarma, D. D.; Bencok, P.; Stanescu, S.; et.al., Supramolecular control of the magnetic anisotropy in two-dimensional high-spin Fe arrays at a metal interface. *Nature Materials* **2009**, *8*, 189–193.

(8) Tseng, T.-C.; Lin, C.; Shi, X.; Tait, S. L.; Liu, X.; Starke, U.; Lin, N.; Zhang, R.; Minot, C.; Hove, M. A. V.; et.al., Two-dimensional metal-organic coordination networks

of Mn-7,7,8,8-tetracyanoquinodimethane assembled on Cu(100): Structural, electronic, and magnetic properties. *Phys. Rev. B* **2009**, *80*, 155458.

(9) Fabris, S.; Stepanow, S.; Lin, N.; Gambardella, P.; Dmitriev, A.; Honolka, J.; Baroni, S.; Kern, K. Oxygen Dissociation by Concerted Action of Di-Iron Centers in Metal-Organic Coordination Networks at Surfaces: Modeling Non-Heme Iron Enzymes. *Nano Lett* **2011**, *11*, 5414.

(10) Reichert, J.; Schiffrin, A.; Auwaerter, W.; Weber-Bargioni, A.; Marschall, M.; Dell'Angela, M.; Cvetko, D.; Bavdek, G.; Cossaro, A.; Morgante, A.; et.al., l-Tyrosine on Ag(111): Universality of the Amino Acid 2D Zwitterionic Bonding Scheme? *ACS Nano* **2010**, *4*, 1218.

(11) Lipton-Duffin, J.; Miwa, J.; Urquhart, S.; Contini, G.; Cossaro, A.; Casalis, L.; Barth, J.; Floreano, L.; Morgante, A.; Rosei, F. Binding Geometry of Hydrogen-Bonded Chain Motif in Self-Assembled Gratings and Layers on Ag(111). *Langmuir* **2012**, *28*, 14291.

(12) Stepanow, S.; Strunskus, T.; Lingenfelder, M.; Dmitriev, A.; Spillmann, H.; Lin, N.; Barth, J.; Wöll, C.; Kern, K. Deprotonation-Driven Phase Transformations in Terephthalic Acid Self-Assembly on Cu(100). *J. Phys. Chem. B* **2004**, *108*, 19392–19397.

(13) Ge, Y.; Adler, H.; Theertham, A.; Kesmodel, L. L.; Tait, S. L. Adsorption and Bonding of First Layer and Bilayer Terephthalic Acid on the Cu(100) Surface by High-Resolution Electron Energy Loss Spectroscopy. *Langmuir* **2010**, *26*, 16325–16329.

(14) Fuhr, J.; Carrera, A.; Murillo-Quirós, N.; Cristina, L. J.; Cossaro, A.; Verdini, A.; Floreano, L.; Gayone, J. E.; Ascolani, H. Interplay between Hydrogen Bonding and Molecular-Substrate Interactions in the Case of Terephthalic Acid Molecules on Cu(001) Surfaces. *J. Phys. Chem. C* **2013**, *117*, 1287.

(15) Tseng, T.-C.; Urban, C.; Wang, Y.; Otero, R.; Tait, S. L.; Alcamí, M.; Écija, D.; Trelka, M.; Gallego, J. M.; Lin, N.; et.al., Charge-transfer-induced structural rearrangements at both sides of organic/metal interfaces. *Nature Chemistry* **2010**, *2*, 374–379.

(16) Peck, J. W.; Koel, B. E. Selective Dehydrogenation of 1,3-Cyclohexadiene on Ordered Sn/Pt(111) Surface Alloys. *Journal of the American Chemical Society* **1996**, *118*.

(17) Peck, J. W.; Mahon, D. I.; Koel, B. E. A temperature programmed desorption study of the reaction of methylacetylene on Pt(111) and Sn/Pt(111) surface alloys. *Surface Science* **1998**, *410*, 200–213.

(18) Panja, C.; Saliba, N. A.; Koel, B. E. Acetylene Chemisorption on Sn/Pt(100) Alloys. *Journal of Physical Chemistry B* **2001**, *105*, 3786–3796.

(19) Zhao, H.; Kim, J.; Koel, B. E. Adsorption and reaction of acetaldehyde on Pt(111) and Sn/Pt(111) surface alloys. *Surface Science* **2003**, *538*, 147–159.

(20) Panja, C.; Samano, E.; Saliba, N. A.; Koel, B. E. Probing the chemistry of CH_3I on Pt/Sn alloys. *Surface Science* **2004**, *553*, 39–49.

(21) Kim, J.; Welch, L. A.; Olivas, A.; Podkolzin, S. G.; Koel, B. E. Adsorption and Decomposition of Cyclohexanone ($C_6H_{10}O$) on Pt(111) and the (2×2) and ($\sqrt{3} \times \sqrt{3}$)R30°-Sn/Pt(111) Surface Alloys. *Langmuir* **2010**, *26*, 16401–16411.

(22) Ma, H.-Y.; Wang, G.-C. Theoretical study of 1,3-cyclohexadiene dehydrogenation on Pt(111), Pt3Sn/Pt (111), and Pt2Sn/Pt(111) surfaces. *Journal of Catalysis* **2011**, *281*, 63–75.

(23) Gao, J.; Zhao, H.; Yang, X.; Koel, B. E.; Podkolzin, S. G. Controlling Acetylene Adsorption and Reactions on Pt/Sn Catalytic Surfaces. *ACS Catalysis* **2013**, *3*, 1149–1153.

(24) Hamm, G.; Schmidt, T.; Breitbach, J.; Franke, D.; Becker, C.; Wandelt, K. The adsorption of benzene on Pd(111) and ordered Sn/Pd(111) surface alloys. *Surface Science* **2004**, *562*, 170–182.

(25) Breinlich, C.; Haubrich, J.; Becker, C.; Valcárcel, A.; Delbecq, F.; Wandelt, K. Hydrogenation of 1,3-butadiene on Pd(111) and PdSn/Pd(111) surface alloys under UHV conditions. *Journal of Catalysis* **2007**, *251*, 123–130.

(26) Štěpán Pick, Density-functional study of the CO chemisorption on bimetallic PdâĂŞSn(110) surfaces. *Surface Science* **2009**, *603*, 2652–2657.

(27) Martínez-Blanco, J.; Joco, V.; Balasubramanian, T.; Segovia, P.; Michel, E. G. Surface phase diagram and temperature induced phase transitions of Sn/Cu(1 0 0). *App. Surf. Sci.* **2006**, *252*, 5331.

(28) Fuhr, J. D.; Gayone, J. E.; Martínez-Blanco, J.; Michel, E. G.; Ascolani, H. Structural and electronic properties of $(3\sqrt{2} \times \sqrt{2})R45°$:a DFT and STM study. *Physical Review B* **2009**, *80*, 115410.

(29) Martínez-Blanco, J.; Joco, V.; Ascolani, H.; Tejeda, A.; Quirós, C.; Panaccione, G.; Balasubramanian, T.; Segovia, P.; Michel, E. G. Fermi surface gapping and nesting in the surface phase transition of SnâĹŢCu(100). *Phys. Rev. B* **2005**, *72*, 041401(R).

(30) Gayone, J. E.; Carrera, A.; Grizzi, O.; Bengió, S.; Sánchez, E. A.; Martínez-Blanco, J.; Michel, E. G.; Fuhr, J. D.; Ascolani, H. Order-disorder phase transition of vacancies in surfaces: the case of Sn/Cu(001)-0.5 ML. *Physical Review B* **2010**, *82*, 035420.

(31) Stepanow, S.; Ohmann, R.; Leroy, F.; Lin, N.; Strunskus, T.; Wo, C.; Kern, K. Rational Design of Two-Dimensional Nanoscale Networks by Electrostatic Interactions at Surfaces. *ACS Nano* **2010**, *4*, 1813–1820.

(32) Clair, S.; Pons, S.; Seitsonen, A. P.; Brune, H.; Kern, K.; Barth, J. STM Study of Terephthalic Acid Self-Assembly on Au(111): Hydrogen-Bonded Sheets on an Inhomogeneous Substrate. *J. Phys. Chem. B* **2004**, *108*, 14585–14590.

(33) Cossaro, A.; Puppin, M.; Cvetko, D.; Floreano, L. Amino-carboxylic recognition on surfaces: from 2D to 2D + 1 nano-architectures. *Phys. Chem. Chem. Phys.* **2012**, *14*, 13154.

(34) Zhang, W.; Nefedov, A.; Naboka, M.; Caob, L.; Wöll, C. Molecular orientation of terephthalic acid assembly on epitaxial graphene: NEXAFS and XPS study. *Phys. Chem. Chem. Phys.* **2012**, *14*, 10125–10131.

(35) Floreano, L.; Cossaro, A.; Gotter, R.; Verdini, A.; Bavdek, G.; Evangelista, F.; Ruocco, A.; Morgante, A.; Cvetko, D. Periodic Arrays of Cu-Phthalocyanine Chains on Au(110). *J. Phys. Chem. C* **2008**, *112*, 10794.

(36) Cautero, G.; Sergo, R.; Stebel, L.; Lacovig, P.; Pittana, P.; Pedronzani, M.; Carrato, S. A two-dimensional detector for pump-and-probe and time resolved experiments. *Nucl. Instrum. Methods Phys. Res. A* **2008**, *595*, 447–459.

(37) Floreano, L.; Naletto, G.; Cvetko, D.; Gotter, R.; Malvezzi, M.; Marassi, L.; Morgante, A.; Santaniello, A.; Verdini, A.; Tommasini, F.; et.al., Performance of the grating-crystal monochromator of the ALOISA beamline at the Elettra Synchrotron. *Rev. Sci. Instrum.* **1999**, *70*, 3855–3865.

(38) Giannozzi, P.; Baroni, S.; Bonini, N.; Calandra, M.; Car, R.; Cavazzoni, C.; Ceresoli, D.; Chiarotti, G. L.; Cococcioni, M.; Dabo, I.; et.al., QUANTUM ESPRESSO: a modular and open-source software project for quantum simulations of materials. *J. Phys.: Condens. Matter* **2009**, *21*, 395502.

(39) Dion, M.; Rydberg, H.; Schroder, E.; Langreth, D. C.; Lundqvist, B. I. Van der Waals Density Functional for General Geometries. *Phys. Rev. Lett.* **2004**, *92*, 246401.

(40) Thonhauser, T.; Cooper, V. R.; S. Li, A. P.; Hyldgaard, P.; Langreth, D. C. Van der Waals density functional: Self-consistent potential and the nature of the van der Waals bond. *Phys. Rev. B* **2007**, *76*, 125112.

(41) Roman-Perez, G.; Soler, J. M. Efficient Implementation of a van der Waals Density Functional: Application to Double-Wall Carbon Nanotubes. *Phys. Rev. Lett.* **2009**, *103*, 096102.

(42) Lee, K.; Murray, É. D.; Kong, L.; Lundqvist, B. I.; ; Langreth, D. C. Higher-accuracy van der Waals density functional. *Phys. Rev. B* **2010**, *82*, 081101.

(43) Cooper, V. R. Van der Waals density functional: An appropriate exchange functional. *Phys. Rev. B* **2010**, *81*, 161104.

(44) Bisti, F.; Stroppa, A.; Perrozzi, F.; Donarelli, M.; Picozzi, S.; Coreno, M.; Simone, M. D.; Prince, K. C.; Ottaviano, L. The electronic structure of gas phase croconic acid compared to the condensed phase: More insight into the hydrogen bond interaction. *J. Chem. Phys.* **2013**, *138*, 014308.

(45) Cossaro, A.; Puppin, M.; Cvetko, D.; Kladnik, G.; Verdini, A.; Coreno, M.; de Simone, M.; Floreano, L.; Morgante, A. Tailoring SAM-on-SAM Formation. *J. Phys. Chem. Lett.* **2011**, *2*, 3124–3129.

(46) We found solid evidences that the substrate transition does not play any significant role in the desorption process. Concretely, we performed complementary desorption experiments (using ion-scattering spectroscopy) with a much lower heating rate (2 K/min). In this case, the desorption temperature is shifted to 345 K, as predicted by the first-order Polanyi-Wigner law when the desorption energy and frequency factor values reported in the text are used. L.J. Cristina et al., to be published.

(47) Paserba, K. R.; Gellman, A. J. Kinetics and Energetics of Oligomer Desorption from Surfaces. *Physical Review Letters* **2001**, *86*, 4338–4341.

(48) Tait, S. L.; Dohnalek, Z.; Campbell, C. T.; Kay, B. D. n-alkanes on MgO(100). II. Chain length dependence of kinetic desorption parameters for small n-alkanes. *J. Chem. Phys* **2005**, *122*, 164708.

(49) Demirci, E.; Winkler, A. Condensation and desorption of nickel tetra-carbonyl on Cu(1 1 0). *Surface Science* **2009**, *603*, 3068–3071.

(50) Stöhr, J. *NEXAFS Spectroscopy*; Springer, 2003.

(51) Bailey, M.; Brown, C. J. The Crystal Structure of Therephthalic Acid. *Acta Cryst.* **1967**, *22*, 387–391.

(52) Ferrighi, L.; Madsen, G. K.; Hammer, B. Self-consistent meta-generalized gradient approximation study of adsorption of aromatic molecules on noble metal surfaces. *J. Chem. Phys.* **2011**, *135*, 084704.

(53) Syomin, D.; Kim, J.; Koel, B.; Ellison, G. Identification of Adsorbed Phenyl (C6H5) Groups on Metal Surfaces: Electron-Induced Dissociation of Benzene on Au(111). *J. Phys. Chem. B* **2001**, *105*, 8387–8394.

(54) Dmitriev, A.; Lin, N.; Weckesser, J.; Barth, J. V.; Kern, K. Supramolecular Assemblies of Trimesic Acid on a Cu(100) Surface. *J. Phys. Chem. B* **2002**, *106*, 6907.

(55) Cheng, Y. Y.; Sun, W.; Wang, Y.; Shao, X.; Xu, X.; Cheng, F.; Li, J.; Wu, K. A Unified Model: Self-Assembly of Trimesic Acid on Gold. *J. Phys. Chem. C Lett.* **2007**, *111*, 10138–10141.

TOC Figure